Damped flexure of a plate above a viscous mantle - postglacial rebound in SW Coastal BC

December 22, 2021

Francis Rossmann
Final Project for EOSC 543 Basin Analysis

1 Introduction

The Cordilleran ice sheet was the smaller of the two continental ice sheets that covered North America during Quaternary glacial periods. The weight of the over-riding ice sheet caused tens to hundreds of meters of crustal displacement along the coastal region of southwestern British Columbia (Clague, 1980). The Cordilleran ice sheet induces the surface of the Earth to experience a significant flexure due to the massive surface loading from the ice load. Beneath and immediately adjacent to the ice sheet, the surface experiences a negative vertical displacement (subsidence) while at the peripheries, a forebulge is created by positive vertical displacement of the crust (Allen and Allen, 2013). The flexural response of the crust under this loading is damped by the flow of the underlying mantle away from occurs on relatively short geological timescales (Wangen, 2010). Following its rapid retreat after the last glacial maximum, the unloaded crust quickly rebounded due to glacial isostatic adjustment (GIA) as the crust and mantle return to an equilibrium state and leading to a rapidly decreasing relative sea level (RSL) in the region. The duration of this response is largely dependent on the viscosity of the underlying mantle and the thickness of the lithosphere. Sea level change due largely to GIA can therefore provide information on the rheology of the Earth's mantle, as the characteristic timescale of GIA is modulated by the rheological properties of the underlying mantle which dampens the flexural response. Here, we use a 2D viscous half space model to investigate the GIA in southwestern coastal British Columbia following to the retreat of the Cordilleran ice sheet after the Last Glacial Maximum. Well constrained sea-level histories compiled from radiocarbon dates for the Fraser Valley and northern Strait of Georgia are used to model the rheology of the mantle in southwestern British Columbia.

2 Regional setting

This study examines fluctuations in relative sea level over the late Quaternary along the north and south-east boundary of the Strait of Georgia in British Columbia. Specifically, I consider the Lower Mainland/ Fraser Valley and the Discovery Islands at the north end of the Strait of Georgia between the British Columbia mainland and Vancouver Island. The tectonic regime in this coastal region is characterized by the Cascadia subduction zone, controlled mainly by the motions of the Pacific, North American, Juan de Fuca and smaller Explorer microplate (Mazzotti et al., 2003). The oceanic Juan de Fuca plate subducts beneath the North American plate at a rate of about 4 cm/annum (Riddihough, 1984). Surface heat flow in this region is also low suggesting the presence

of a stagnant and cool mantle wedge (Hyndman and Lewis, 1995). Previous studies have used relative sea level and relict lake-shoreline tilt observations to indicate that the viscosity of the shallow mantle is low in comparison to adjacent cratonic regions (e.g., Matthews et al., 1970).
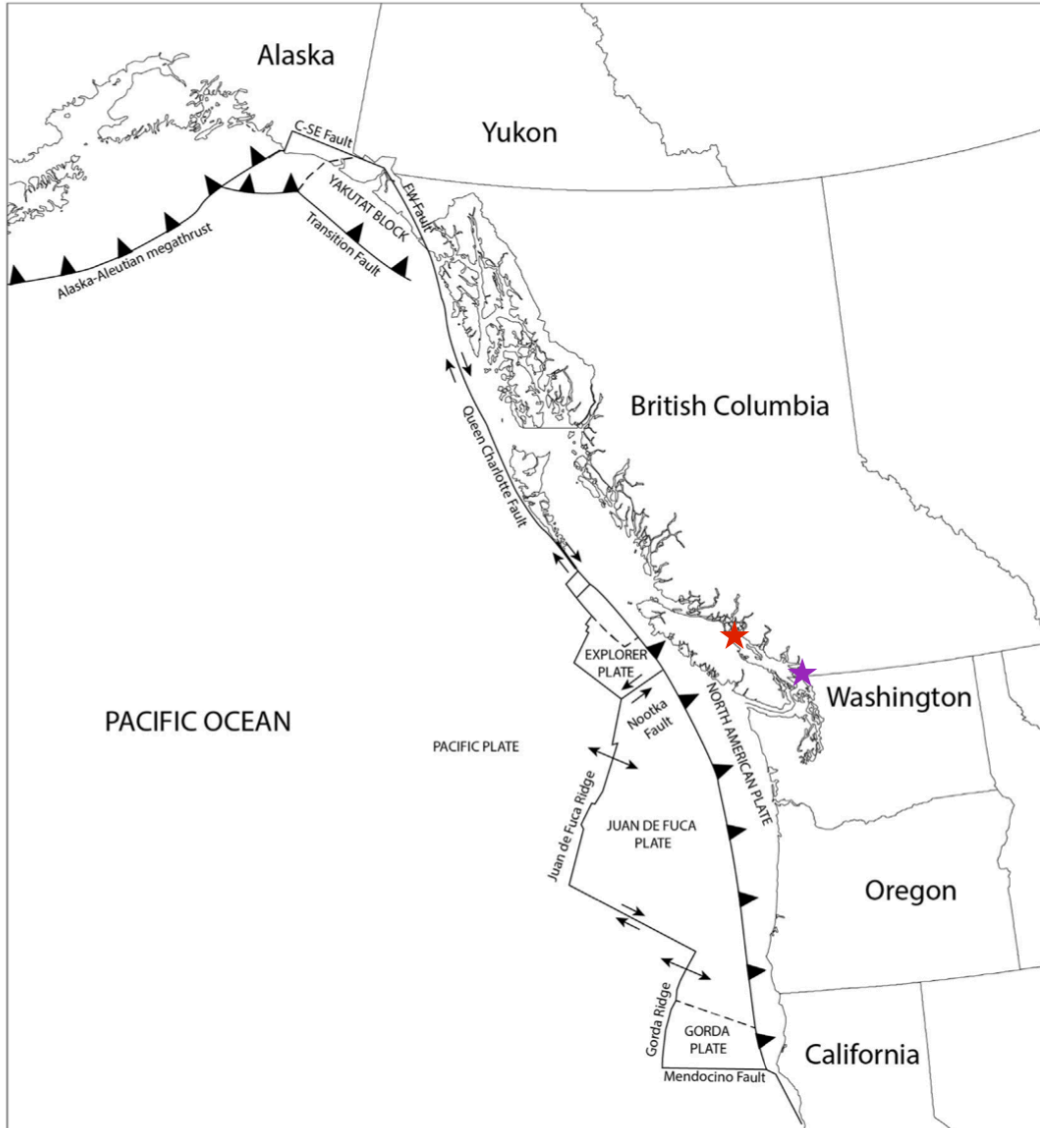

Figure 1: Map of the study region showing tectonic regime of the area of study. The lower Fraser valley is shown by a magenta star, and the northern Strait of Georgia is indicated by a red star. Adapted from Shugar, 2014.

The northern Cascadia region examined here represents a portion of the Cascadia subduction zone that experienced the highest extent of glaciation (Shugar, 2014) under the Cordilleran ice sheet. The (Late Wisconsinan) Fraser glaciation is the last glaciation period that occupied most of southwestern British Columbia, including coverage of the Strait of Georgia. The maximum extent of the Fraser glaciation ocurred approximately 17-16 kyr ago (Clague & James, 2002). The areal coverage of the Cordilleran ice sheet at its maximum is estimated to be about 1.5 million km^2 with a

width of about 900km as interpreted from glacial meltwater landforms (Margold, 2013). By 14 kyr ago, the Cordilleran ice sheet had retreated to the northern end of the Strait (Barrie and Conway, 2002). Peak ice thickness in the Strait of Georgia is estimated to have been about 2km during this stage. By about 13.7 kyr before present, the Strait of Georgia was largely ice free although from 12.7-12.9 kyr ago during the Older and Younger Dryas, there were several glacier advances to the north (Shugar, 2014). Rapid deglaciation along the edges of the Cordilleran ice sheet led to isostatic adjustment and drops in relative sea level in this region (e.g., Matthews et al., 1970; James et al., 2009). The Pleistocene shorelines along southwestern British Columbia vary due to the variable timing of glacial isostatic adjustment (GIA) following retreat of the Cordilleran ice sheet after the last glacial maximum (LGM). Previous studies have shown that relative sea level in this region has fallen rapidly from a highstand position about 13.5-14 kyr ago (James et al., 2005).

3 Method

Ice sheet loads force the underlying mantle to flow laterally to create space for the flexurally subsiding crust. A rapidly loaded elastic plate does not instantly deflect under load because of the viscous damping that the underlying ductile mantle provides. Mountain building occurs over long timescales, so dynamic effects can be neglected, and the mantle is assumed to be in hydrostatic equilibrium throughout the process. Ice sheet growth and melt occurs on much shorter timescales where dynamic effects become more important. To investigate the response of the Earth's mantle to the removal of an ice load, we consider a simplified model for flow in a semi-infinite, viscous fluid half-space which is subjected to an initial periodic surface displacement due to surface load from glaciation as described in Turcotte & Schubert (2018). The initial periodic surface displacement is assumed to take the form:

$$w_m = w_{mo} \cos(2\pi x/\lambda)$$

Where w_{mo} is the maximum initial displacement and λ is the wavelength of the ice sheet.

Upon unloading the surface, the return of the surface to an undeformed state is governed by the viscous flow of the mantle in the half-space. For an incompressible two-dimensional viscous fluid flow, the stream function, ψ, which represents the volumetric flow rate between any two points satisfies the biharmonic function $\nabla^4 \psi = 0$. The stream function is defined such that: $u = -\frac{\partial \psi}{\partial y}$ in the y direction, and $v = \frac{\partial \psi}{\partial x}$ in the x-direction.

We can assume that the solution for ψ is directly proportional to either $\sin(2\pi x/\lambda)$ or $\cos(2\pi x/\lambda)$ and solve this PDE with separation of variables assuming a solution of the form $\psi = \sin(\frac{2\pi x}{\lambda})Y(y)$ for some $Y(y)$. Boundary conditions for this problem require the solution to be finite as $y \to \infty$, and we enforce a no-slip condition at the upper boundary of the fluid half space. The final boundary condition is set such that the hydrostatic pressure head associated with topography is equal to the normal stress at the upper boundary of the fluid half space. Full integration of this problem after separation of variables yields a time-dependent solution for flexure with the form:

$$w = w_{mo} \exp\left(\frac{-\lambda \rho g t}{4\pi\mu}\right)$$

We see the surface displacement decreases exponentially with time as fluid flows from regions of elevated topography to regions of depressed topography. We can let $\tau_r = \frac{4\pi\mu}{\rho g \lambda}$ and write the solution

as:

$$w = w_{mo}e^{-t/\tau_r}$$

Where τ_r is the characteristic time scale for the exponential relaxation (e-folding timescale) of the initial displacement profile. Clearly, we can see that the time to rebound from some initial deflection is faster for short wavelength loads. In this model, a lower viscosity also results in a faster rebound timescale. After determining the characteristic timescale τ_r for post-glacial rebound, we can solve for the underlying mantle viscosity μ:

$$\mu = \frac{\rho g \lambda \tau_r}{4\pi}$$

For this problem, an ice sheet wavelength of $\lambda = 900km$ is assumed for the Cordilleran ice sheet following the maximum ice sheet width given in Margold (2013). Mantle viscosity is taken as $rho_m = 3300kgm^{-3}$. Relative sea level fall is assumed to initiate at 14 kyr ago, consistent with the timing of deglaciation in the region (James, 2005).

4 Data

Quantitative constraints on the rate of postglacial rebound can be obtained from relative sea level data. Relative sea level data for this study is collected from a database of sea-level points, sea-level datums, and dating conventions provided by Shugar et al. (2014) as supplementary data. This database uses numerous sea level indicators compiled from previously published sources. Metadata for each entry include the site name, latitude/longitude, type of material sampled, published 14C age with uncertainty, sample elevation and uncertainty (corrected for mean sea-level), and geographic region. Relevant information for the Fraser valley mainland and northern Strait of Georgia are retrieved from the database for analysis. The relative sea level change of these sites is compared with the exponential relaxation curves described above. The value of the characteristic time corresponding to the qualitatively best fitting curves is then used to constrain a viscosity estimate for the underlying mantle.

For the Fraser valley, data is compiled from Clague (1980), Easterbrook (1963), Hutchinson (1992), Dethier et al (1995), Mathews et al (1970), and James et al (2002) for a total of 227 independent observations. Data for the northern Strait of Georgia is compiled from Hutchinson (1992), James et al (2005), and partially compiled from Fedje (2018) using core-logged data from isolation basins only. For the purposes of this study, we combine the isolation basin core results from Fedje (2018) with the results from Hutchinson (1992) and James et al. (2005).

Reported elevations in this paper are relative to present day sea level and have not had any additional corrections applied to them.

5 Results

The solution GIA curves for a 2D viscous mantle half-space are computed for a variety of different candidate viscosities. Viscosities considered here are 1×10^{19}, 5×10^{19}, 1×10^{20}, and 2×10^{20} Pa s. The characteristic exponential folding time of the curve is set by the timescale parameter τ_r which is proportional to the dynamic viscosity of the mantle as shown in the *Methods* section. Then,

we compare the distributions of paleo-sea-levels in the Fraser Valley mainland and north Strait of Georgia to these relaxation curves to constrain a reasonable range of mantle viscosities which describe the observed response well.
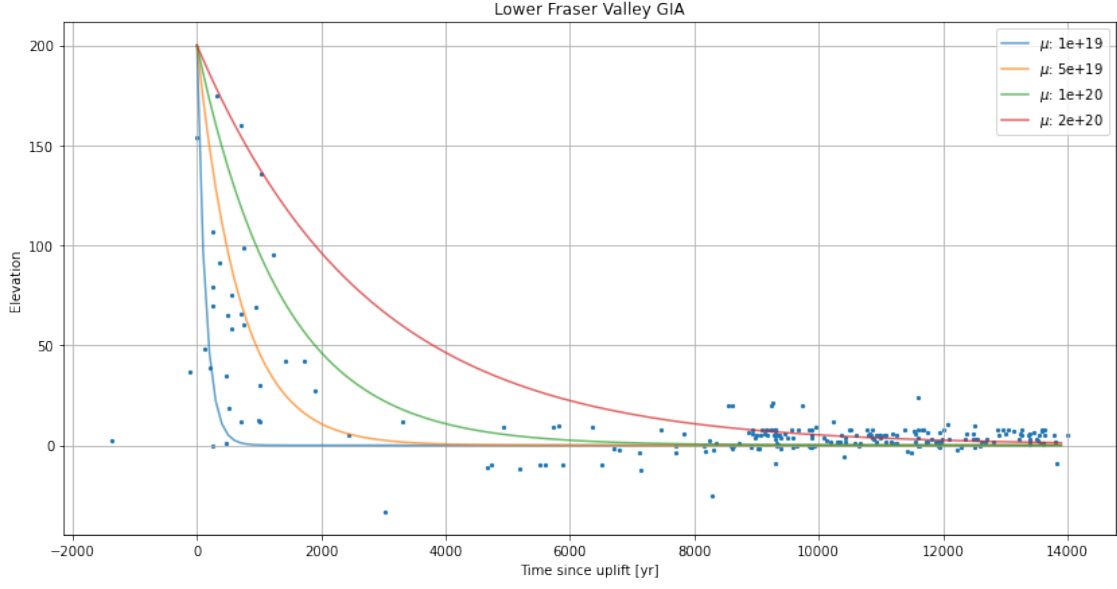

Figure 2: Relative sea level scatter for the lower Fraser valley obtained from the RSL database in Shugar (2014). Four relaxation curves as parametrized in the *Methods* section are shown for a range of characteristic timescales governed by the mantle viscosity.

Figure 3: Relative sea level scatter for the northern Strait of Georgia obtained from the RSL database in Shugar (2014) and isolation basin cores taken in Fedje (2018). Orange points correspond to observations from Fedje (2018) and blue points are from Hutchinson (1992) and James et

al. (2005). Four relaxation curves as parametrized in the *Methods* section are shown for a range of characteristic timescales governed by the mantle viscosity.
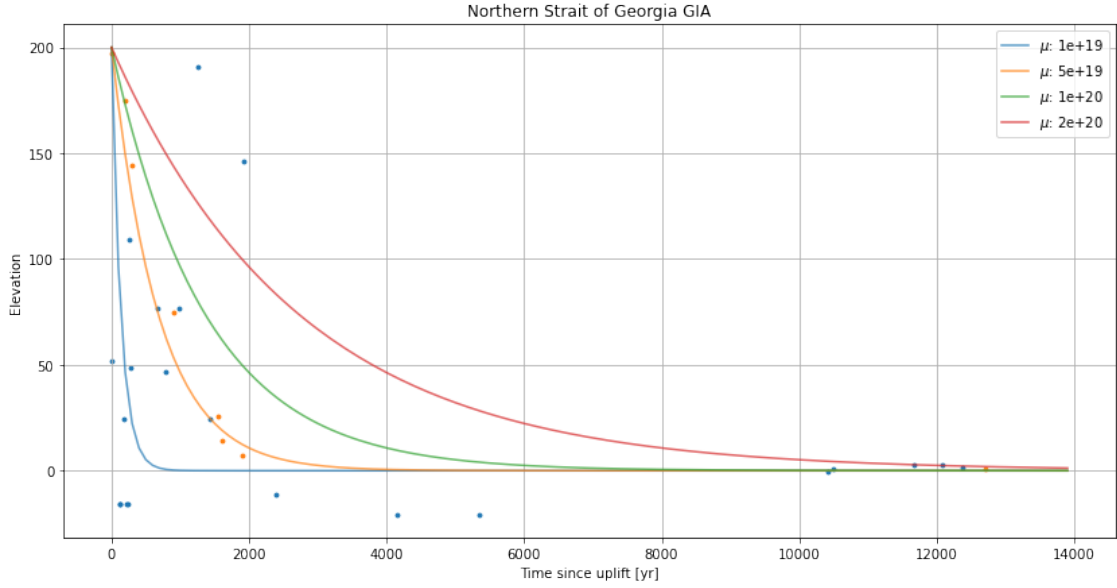
——

Figures 2 and 3 show the selected paleo relative sea level data as a scatter plot for the Fraser valley mainland and Discovery islands (respectively). The sea level scatter is superposed with the exponential relaxation curves computed for a range of candidate mantle viscosities (described in the Methods section). The relative sea level scatters for both the lower Fraser valley and the northern Strait of Georgia fall below zero metres above sea level, while the relaxation curve is limited to take on only positive values. We can qualitatively assess the appropriate relaxation curves to describe this problem by identifying the envelope of curves which enclose the elevation data. We find good qualitative fit to uplift-age data for a range of mantle viscosities on the order of magnitude of 1×10^{19} to 1×10^{20} Pa s. The lower range of the viscosities examined here is given by a viscosity of 1×10^{19} Pa s, for which the relaxation curve appears to decay faster than the rate at which GIA induced uplift occurs. Due to scatter in the RSL data, it is not immediately clear which mantle viscosity best describes the rate at which the GIA response occurs at. While a metric to evaluate the goodness of fit is certainly possible, caution should be taken due to limitations of the viscous dampening model examined here (detailed in the discussion below). We can, however, see that the observed relaxation time is too fast to imply a high viscosity mantle above 1×10^{20} Pa s, and that the observed elevations are best described by a range of mantle viscosities between 1×10^{19} and 1×10^{20} Pa s.

6 Discussion

The results are generally in agreement with other studies showing a low mantle viscosity on the order of 10^{19} Pa s in the Cascadia subduction zone (e.g. James, 2000; Clague and James, 2002). However, more recent studies show that these results may be a slight overestimate. For example, GIA modelling by James (2009) found an optimum value for aesthenosphere viscosity ranging from 3×10^{18} Pa s to 4×10^{19} Pa s . Limitations of the uniformly viscous half-space model employed here are likely responsible for this overestimate. For example, while the model used here is simple to solve, a layered rheology has been shown to be more realistic for the Earth (e.g., McConnell, 1965) and the solution for a model such as this one yield decay times for each shell boundary which can be integrated for a net surface response. In any case, a uniformly viscous half space may not adequately describe the complex rheology of this setting.

Additionally, constraints on the extent and loading of the Cordilleran ice sheet may inform the overestimate of mantle viscosity seen here. For example, the wavelength which best describes the ice sheet used in this analysis ($\lambda = 900 km$) is merely an estimate and does not accurately describe the geometry of the ice sheet. Furthermore, the distribution of the ice sheet load was not spatially geometrically homogenous as assumed here, and the near-field GIA response of the uplifting crust has been shown to be heterogenous in space (Shugar, 2014).

Finally, changes in relative sea level are the result of many oceanic and crustal processes that act at a range of temporal and spatial scales (Nelson et al. 1996). The late Pleistocene shoreline along the Pacific coast of Canada has responded to the retreat and thinning of the Cordilleran ice sheet (e.g., Clague et al., 1982; McLaren et al., 2014), leaving behind a quantifiable record of relative sea level change. However, the observed changes in relative sea level shown in Figures 2 and 3 are likely not only due to glacial isostatic adjustments only. For example, this region includes the northern limit of plate rupture which yielded the AD 1700 subduction earthquake (Benson et al., 1999)

which has been noted to induce some degree of co-seismic slumping and subsidence in the region. Other crustal factors including deformation and sedimentation likely all contribute to changes in RSL which are not considered here. However, it is worth noting that the observed magnitudes of relative sea level adjustment here are generally too large to be explained by anything other than glacially induced isostatic rebound and eustasy (Shugar, 2014). Nevertheless, while the relative sea level scatters in Figures 2 and 3 for both the lower Fraser valley and the northern Strait of Georgia can be seen to take on negative values relative to the mean sea level today, the fit of the relaxation curve is still useful for the qualitative interpretation of the rate at which relative sea level changes take place. This point can be addressed in future work by correcting the relative sea level data used here for global eustatic adjustments for a more accurate measure of GIA induced uplift.

7 Conclusion

In the above, we have solved the postglacial rebound problem in a two-dimensional Cartesian geometry for a region in the southwestern coast of British Columbia in the lower Fraser valley and northern Strait of Georgia. We see that the best fit mantle viscosity obtained using the approximate analytical solution is in good agreement with past literature. A more rigorous approach to this problem can be investigated by modelling the Earth as a series of concentric shells each with their own uniform properties (e.g., viscosity and density). Thus, more complete studies of postglacial rebound should consider the flexural rigidity of the elastic lithosphere, and a depth dependant (layered) mantle viscosity. It is recommended that a three-dimensional multi-layered rheological model is used to investigate the GIA response more accurately in this region. Additionally, more precise constraints on relative sea level changes in the region can be used in the future to more rigourously investigate this problem. Finally, more accurate constraints on the extent and size of the Cordilleran ice sheet during and after the Last Glacial Maximum prior to deglaciation will allow for a more accurate description of the GIA induced uplift studied here.

8 References

Allen, Philip A.; Allen, John R., 2013. Basin Analysis. Hoboken, NJ: Wiley-Blackwell.

Benson, B.E., Clague, J.J., Grimm, K.A., 1999. Relative sea-level change inferred from intertidal sediments beneath marshes on Vancouver Island, British Columbia. Quat. Int. 60, 49-54.

Clague, J.J., 1980. Late Quaternary geology and geochronology of British Columbia, part 1: radiocarbon dates. Geological Survey of Canada, Energy Mines and Resources Canada, Paper 80-13, 28.

Clague, J.J. and James, T.S., 2002. History and isostatic effects of the last ice sheet in southern British Columbia. Quaternary Science Reviews, 21, 71-87.

Dethier, D.P., Pessl Jr., F., Keuler, R.F., Balzarini, M.A. and Pevear, D.R., 1995. Late Wisconsinian glaciomarine deposition and isostatic rebound, northern Puget Lowland, Washington. GSA Bulletin, 107, 1288-1303.

Easterbrook, D.J., 1992. Advance and retreat of Cordilleran ice sheets in Washington, U.S.A. Géographie Physique et Quaternaire, 46, 51-68.

Fedje, Daryl et al, 2018. "A revised sea level history for the northern Strait of Georgia, British Columbia, Canada." Quaternary Science Reviews.

Gowan, E.J., 2007. GLACIO-ISOSTATIC ADJUSTMENT MODELLING OF IMPROVED RELATIVE SEA-LEVEL OBSERVATIONS IN SOUTHWESTERN BRITISH COLUMBIA, CANADA. University of Victoria, Thesis.

Hutchinson, I., 1992. Holocene sea level change in the Pacific Northwest: a catalogue of radiocarbon dates and an atlas of regional sea-level curves. Occasional Paper No. 1, Institute of Quaternary Research, Simon Fraser University, Burnaby, B.C., 100 p.

Hyndman R.D., Lewis, T. J., (1995). Review: The thermal regime along the southern Canadian Cordillera Lithoprobe corridor. Canadian Journal of Earth Sciences. 32(10): 1611-1617.

James, T.S., Clague, J.J., Wang, K. and Hutchinson, I., 2000. Postglacial rebound at the northern Cascadia subduction zone. Quaternary Science Reviews, 19, 1527-1541.

James, T.S., Hutchinson, I., Barrie, J.V., Conway, K.C. and Mathews, D., 2005. Relative sea-level change in the northern Strait of Georgia, British Columbia. Géographie Physique et Quaternaire, 59, 113-127.

James, T.S., Hutchinson, I. and Clague, J.J., 2002. Improved relative sea-level histories for Victoria and Vancouver, British Columbia, from isolation-basin coring. Geological Survey of Canada, Current Research 2002-A16, Natural Resources Canada, 7.

James, T.S., 2009. Viscosity of the asthenosphere from glacial isostatic adjustment and subduction dynamics at the northern Cascadia subduction zone, British Columbia, Canada, JGR, 114-B4.

Margold, M., Jansson, K. N., Kleman, J., Stroeven, A. P. & Clague, J. J. 2013. Retreat pattern of the Cordilleran Ice Sheet in central British Columbia at the end of the last glaciation reconstructed from glacial meltwater landforms. Boreas, Vol. 42, pp. 830–847.

Mathews, W.H., Fyles, J.G. and Nasmith, H.W., 1970. Postglacial crustal movements in southwestern British Columbia and adjacent Washington state. Canadian Journal of Earth Sciences, 7, 690-702.

Mazzotti, S., Dragert, H., Henton, J., Schmidt, M., Hyndman, R., James, T., Lu, Y. and Craymer, M., 2003. Current tectonics of northern Cascadia from a decade of GPS measurements. Journal of Geophysical Research, 108, 2554

McConnell, R.K., 1965. Isostatic adjustment in a layered Earth. Journal of Geophysical Research, 70, 5171-5188

McLaren, D., Fedje, D., Hay, M., Mackie, Q., Walker, I.J., Shugar, D.H., Eamer, J.B.R., Lian, O.B., Neudorf, C., 2014. A post-glacial sea level hinge on the central Pacific coast of Canada. Quat. Sci. Rev. 97, 148-169.

Nelson, A.R., Shennan, I., Long, A.J., 1996. Identifying coseismic subsidence in tidal- wetland stratigraphic sequences at the Cascadia subduction zone of western North America. J. Geophys. Res. 101.

Riddihough, R., 1984. Recent movements of the Juan de Fuca plate system. Journal of Geophysical Research, 89, 6980-6994.

Shugar, D.H. et al, 2014. Post-glacial sea-level change along the Pacific coast of North America, Quaternary Science Reviews, 97, 170-192.

Turcotte, D., & Schubert, G., 2014. Geodynamics (3rd ed.). Cambridge: Cambridge University Press.

Wangen, Magnus, 2010. Physical Principles of Sedimentary Basin Analysis, Cambridge Core: Cambridge University Press.